Biological Psychology 169 (2022) 108277

Contents lists available at ScienceDirect

Biological Psychology

journal homepage: www.elsevier.com/locate/biopsycho

Neural substrates of respiratory sensory gating: A human fMRI study

Pei-Ying S. Chan [a,b,*], Chia-Hsiung Cheng [a,b,c], Yu-Ting Wu [a,b], Changwei W. Wu [d,e,**], Ai-Ling Hsu [f], Chia-Yih Liu [b], Ho-Ling Liu [g], Paul W. Davenport [h]

[a] Department of Occupational Therapy and Healthy Aging Center, Chang Gung University, Taoyuan, Taiwan
[b] Department of Psychiatry, Chang Gung Memorial Hospital at Linkou, Taoyuan, Taiwan
[c] Laboratory of Brain Imaging and Neural Dynamics (BIND Lab), Chang Gung University, Taoyuan, Taiwan
[d] Graduate Institute of Mind, Brain and Consciousness, Taipei Medical University, Taipei, Taiwan
[e] Brain and Consciousness Research Center, Shuang-Ho Hospital, Taipei Medical University, New Taipei, Taiwan
[f] Bachelor Program in Artificial Intelligence, Chang Gung University, Taoyuan, Taiwan
[g] Department of Imaging Physics, The University of Texas MD Anderson Cancer Center, Houston, TX, United States
[h] Department of Physiological Sciences, The University of Florida, Gainesville, FL, United States

ARTICLE INFO

Keywords:
Respiratory sensory gating
Human fMRI
Respiratory sensation
Paired inspiratory occlusions
Cortical and subcortical substrates

ABSTRACT

The involvement of neural substrates in respiratory sensory gating remained unclear. This study aimed to investigate cortical and subcortical activations associated with respiratory sensory gating by using functional magnetic resonance imaging. First, we hypothesized that paired occlusions would induce neural activation in cortical and subcortical areas, including the thalamus and sensorimotor cortices. Secondly, we hypothesized that, in terms of parameter estimates in the general linear model, the activation effect size β ratios ($\beta_{paired}/\beta_{single}$) would be less than 2 due to central neural gating mechanism. Forty-six healthy participants were included in the study. Our analyses showed that the βpaired/βsingle ratios for the supramarginal gyrus, basal ganglia, thalamus, and middle frontal gyrus were less than 2. In conclusion, our results demonstrated a non-linear relationship regarding brain neural activations in response to paired versus single occlusions, suggesting that respiratory sensory information is gated at the subcortical and cortical levels.

1. Introduction

Respiratory somatosensation, or awareness of breathing sensations, is thought to be an integrative and gated system (Chan & Davenport, 2008; Davenport & Vovk, 2009). Self-reported descriptions of breathing sensations range from simply being aware of the breaths to a catastrophic or distressful feeling; however, normal breathing is not usually sensed unless there is an attentional state change or a ventilatory status change. This gated system implies that the central nervous system may "filter out" unwanted information and retain essential information elements (Chan & Davenport, 2008, 2010a). If this gating function is intact, the individual can attend to more important sensory input for energy conservation purposes (Arnfred, Eder, Hemmingsen, Glenthoj, & Chen, 2001). This concept is similar to the existing distal and proximal exteroceptive sensory gating theories proposed in the auditory and somatosensory literature, where deficits in sensory gating function have been suggested to lead to sensory flooding of the cortex and altered symptom perception; for example, in patients with schizophrenia (Adler et al., 1982; Arnfred et al., 2001; Braff & Geyer, 1990).

Sensory gating in proximal and distal exteroception can be tested by somatosensory and auditory evoked potentials where paired stimuli are presented with a 500-ms inter-stimulus interval (ISI) (Adler et al., 1982; Thoma et al., 2007). With cortical dipole modeling, auditory and somatosensory evoked potentials give inferences to information processing of auditory and somatosensory stimulus events, respectively. Similarly, respiratory-related evoked potential (RREP) peak components reflect perceptual and cognitive processing of respiratory sensory stimuli. The auditory gating and somatosensory gating are respectively represented by the P50 and N100 peak amplitudes in response to the second stimulus (S2) in proportion to the first stimulus (S1) in temporal proximity. Studies to-date have reported that in healthy individuals, the auditory P50 and somatosensory N100 peak amplitude S2/S1 ratio is much lower than 1.0, indicating a suppressed S2 processing (Adler & Waldo, 1991; Jelincic, Torta, Van Diest, & von Leupoldt, 2021;

* Correspondence to: Department of Occupational Therapy, Chang Gung University, No. 259, Wen Hua 1st Rd. Kuei Shan District, Taoyuan 333, Taiwan.
** Correspondence to: Graduate Institute of Mind, Brain and Consciousness, Taipei Medical University, Taipei, Taiwan.
E-mail addresses: chanp@cgu.edu.tw (P.-Y.S. Chan), sleepbrain@tmu.edu.tw (C.W. Wu).

https://doi.org/10.1016/j.biopsycho.2022.108277
Received 1 April 2021; Received in revised form 20 January 2022; Accepted 20 January 2022
Available online 22 January 2022

Rentzsch, Jockers-Scherubl, Boutros, & Gallinat, 2008; Shen et al., 2020). Although there was not a clear-cut ratio for the indications of health and disease, those with mental illnesses, such as schizophrenia or panic disorder, usually exhibit higher sensory gating ratios compared with healthy controls (Boutros, Korzyukov, Jansen, Feingold, & Bell, 2004; Thoma et al., 2020, 2007). Respiratory sensory gating can also be measured by the paired inspiratory occlusions where two short occlusions are given with a 500-ms ISI within a single inspiration (Chan & Davenport, 2008). Electrophysiological studies have further revealed that in healthy individuals, the RREP N1 peak amplitude S2/S1 ratio is approximately 0.5 (Chan & Davenport, 2009, 2010a).

The source dipole analysis performed by Logie, Colrain, and Webster (1998) suggested that early RREP peak brain substrates for single respiratory occlusions originate from the pre-central and post-central cortices (Logie et al., 1998; von Leupoldt et al., 2010). Using high-density EEG recordings, von Leupoldt et al. (2010) further suggested that longer-latency peaks (N1, P2, and P3) originate from the lateral and midline frontal cortex, sensorimotor cortex, and parietal cortex (Davenport, Colrain, & Hill, 1996; von Leupoldt et al., 2010; Webster & Colrain, 1998, 2000). However, non-invasive human electrophysiological recordings were unable to give inferences to deep structures such as the hippocampus or thalamus due to limitation in spatial resolution.

Neuroimaging research in dyspnea to-date has mostly studied brain substrates using chemoreceptor or mechanoreceptor stimuli (Banzett et al., 2000; Manning et al., 1992; Moosavi et al., 2003; Peiffer, Costes, Herve, & Garcia-Larrea, 2008; Peiffer, Poline, Thivard, Aubier, & Samson, 2001; von Leupoldt et al., 2008, 2009). These studies found that aversive stimuli, including resistive loads, hypercapnia, and hypoxia, induce significant neural activation in the thalamus, sensorimotor cortex and limbic structures in healthy participants. A recent fMRI study by Chan et al. (2019) found that single inspiratory obstruction activates a thalamocortical network, including the thalamus, supramarginal gyrus, and frontal cortex, in healthy non-smoking participants (Chan et al., 2018). Similarly, Jack, Kemp, Bimson, Calverley, and Corfield (2010) reported that transient single respiratory obstruction activates the anterior insular cortex, premotor and sensorimotor cortices in patients with idiopathic hyperventilation syndrome, although there was a lack of data from healthy control groups (Jack et al., 2010).

Substantial work has been carried out in the past decade to test neural substrates of auditory sensory gating, mostly focused on electrophysiological methodology (Bak, Glenthoj, Rostrup, Larsson, & Oranje, 2011; Bak, Rostrup, Larsson, Glenthoj, & Oranje, 2014; Grunwald et al., 2003; Mayer et al., 2009). The areas identified as potential neural substrates for auditory paired stimuli, compared to a single stimulus in healthy volunteers, are the medial frontal gyrus, insular cortices, hippocampus, and thalamus (Bak et al., 2011; Mayer et al., 2009). Neuroimaging studies, animal studies and human intracranial studies in patients with epilepsy added to the available neural substrate analyses by increasing spatial resolution or providing invasive preparations (Boutros et al., 2004; Freedman, Adler, Myles-Worsley, Nagamoto, &, Miller, 1996; Korzyukov et al., 2007). Earlier fMRI studies were able to elucidate non-linear relationship between single- and paired-stimulus elicited brain substrates in terms of hemodynamic response function (HRF), but mostly tested with an inter-stimulus interval of slightly shorter than 4 s (Friston, Josephs, Rees, & Turner, 1998; Glover, 1999; Huettel & McCarthy, 2000; Inan, Mitchell, Song, Bizzell, & Belger, 2004). Subsequently, Mayer et al. (2009) tested neural substrates of auditory sensory gating with similar paradigms used in event-related potential studies. By modeling the estimated HRF for paired stimuli, they demonstrated that the auditory cortex, prefrontal cortex, and thalamus are key neural substrates for auditory gating (Mayer et al., 2009).

In contrast, there are few studies on brain substrates associated with respiratory sensory gating. The importance of examining brain substrates regarding respiratory sensory gating lies in the fact that the brain inhibitory mechanism for gating-in or gating-out repetitive respiratory stimuli is essential for perceiving and processing respiratory stimuli (Chan & Davenport, 2010a). Therefore, the purpose of this study was to identify cortical and subcortical substrates related to respiratory sensory gating elicited by paired inspiratory occlusions. We examined the neural activation effect size β values for the brain substrates related to respiratory sensory gating. In the general linear model (GLM) of fMRI analysis, β value is the parameter indicating the level of brain activity temporally changing associated with the independent variables, which is viewed as an approximate index for examination of HRF linearity (Dale & Buckner, 1997). In the present study, beta values indicate the level of activation the specific inspiratory occlusion elicits to the specific brain substrate. Targeting on the spatial location, we first hypothesized that paired occlusions would elicit strong neural activations in cortical and subcortical structures such as the thalamus and sensorimotor cortices. With the previous electrophysiological evidence in sensory gating, we further hypothesized that the ratio of effect size in the paired- versus single-occlusion condition ($\beta_{paired}/\beta_{single}$) would be less than 2, indicating a nonlinearity system as expected in the RREP studies. In terms of self-reports, we hypothesized that the participant would give higher dyspnea rating on the Visual Analogue Scale (VAS) in the paired compared with single occlusion condition.

2. Methods

2.1. Participants

Initially, 63 participants were recruited and completed the experiment; however, during offline analysis we discovered there were excessive head motion artefacts in 17 participants' data. Therefore, these 17 participants were excluded from further analysis. The inclusion criteria for all participants were as follows: (1) the ages of participants were at least 20 years old; (2) participants were willing to perform a pulmonary function test with a standard spirometry device (Cardinal Health Inc., Dublin, OH, USA) and (3) potential participants should pass the minimal requirement of the Forced Expiratory Volume in 1 s (FEV_1) of at least 70% of predicted values. Participants with any of the following conditions were excluded: (1) those with head circumference over 60 cm, (2) those who had a history of cold or cough within the past two weeks before the experiment, (3) those with a history of cardiac or respiratory diseases; (4) those with a history of neurological diseases, (5) individuals who had undergone an operation with metal implants or a pacemaker, or with dental braces or metal dentures, and (6) individuals with claustrophobia. All study procedures were approved by the Institutional Review Board of the Chang Gung Medical foundation. All participants provided their written informed consent prior to the experiment.

2.2. Respiratory occlusion conditions

We used two respiratory occlusion conditions (single and paired occlusions) to elicit brain neural activations. For the single-occlusion condition, a 150-ms inspiratory occlusion was provided every 2–4 breaths randomly for approximately 12 min. For the paired-occlusion condition, paired inspiratory occlusions of 150-ms each with a 500-ms inter-stimulus-interval were provided within a single inspiration every 2–4 breaths randomly for also approximately 12 min. Occlusions were provided at the onset of inspiratory mouth pressure change. Approximately 40 single or paired occlusions were collected under each condition.

2.3. Experiment protocol

Upon completion of the pulmonary function test, the participant laid supine on the scanner with the facemask and earplugs secured before putting the head coil in place. After the standardized structural scan, the

participant was instructed to breathe normally while their breath was interrupted occasionally. One single-occlusion experiment and one paired-occlusion experiment were performed for each participant with the sequence of the two conditions randomized across participants. For dyspnea ratings after each experiment, the participants were asked to rate their feeling of shortness of breath (SOB) using a VAS scale (0 = not at all SOB, and 100 = maximal level of SOB).

2.4. Respiratory apparatus

The respiratory apparatus was similar to that of Chan et al. (2018, 2019) studies (Chan et al., 2019, 2018). Briefly, the participant breathed through a facemask which was connected to a two-way non-rebreathing T-valve (Hans Rudolph Inc., Kansas City, USA). Mouth pressure was monitored with a pressure tubing connected to the center of the T-valve. The pressure tubing was connected to a differential pressure amplifier (1110 series, Hans Rudolph Inc., Kansas City, MO, USA) as well as a signal recording unit (PowerLab, ADInstruments Inc., Bella Vista, NSW, Australia). The inspiratory port of the T-valve was connected to a customized occlusion valve which was located approximately 3 m away from the scanner (Hans Rudolph Inc., Kansas City, USA). The occlusion valve was connected to a pressure tank via a solenoid and customized trigger device outside of the scanner. The experimenter triggered closure of the occlusion valve manually based on real-time monitoring of the participant's mouth pressure.

2.5. Image acquisition

The fMRI study was performed on a 3-T scanner (MAGNETOM Prisma, Siemens Healthineers, Erlangen, Germany) at the Imaging Center for Integrated Body, Mind and Culture Research in the National Taiwan University, Taipei, Taiwan. During the scan, the participants laid supine and their heads were comfortably positioned inside a 20-channel head coil, which was padded with sponges to minimize head motions. During the fMRI experiments, 32 continuous axial slices (3.4-mm thickness) were acquired by a T_2.

* -weighted gradient-echo echo-planar imaging sequence (TR= 2000 ms, TE= 30 ms; flip angle= 90 degrees; parallel imaging factor = 2, matrix= 64 ×64; field of view= 220 ×220 mm). The acquisition time was 12 min in each session.

2.6. Data analysis

The fMRI data were analyzed using SPM8 (http://www.fil.ion.ucl.ac.uk/spm/) and AFNI (Cox, 1996). All images were realigned to the first image, spatially normalized into standard anatomical space based on the Montreal Neurologic Institute template and smoothed with an isotropic Gaussian kernel of 6-mm full-width at half-maximum.

At the first-level, the statistical analysis was performed with GLM, which included two experimental conditions: The single-occlusion condition and the paired-occlusion condition. A high-pass filter with a cut-off of two longest periods was applied. To enhance the timing precision, we further applied the temporal and dispersion derivatives in the GLM. After model estimation, the contrasts of interest were generated on the basis of the ensuing parameter estimates for each participant. The contrasts compared the averaged Blood-Oxygen-Level-Dependent (BOLD) response across the baseline conditions (without occlusions) for each of the two respiratory conditions. At the group level, these contrast images were used to examine the differences in brain activations between single- and the paired-occlusion conditions. The threshold for statistical significance set at $p < .05$, family-wise error rate-corrected (FWE) and cluster size > 20 voxels.

As this was an exploratory study, no formal a priori sample size calculation was performed nor a predetermined regions of interest (ROI) size. The ROI were chosen based on two criteria: (1) the regions of difference from the contrast map in the "Paired minus Single" activation results, and (2) the overlapping areas of brain activations in both single and paired-occlusion conditions. The effect size β values were extracted for every chosen ROI in each condition, and the β ratios (β values in paired occlusion condition versus single occlusion condition, $\beta_{paired}/\beta_{single}$) were also calculated. Originally, the beta ratios were planned to being compared with the values of 2 with one sample T-test under the superposition assumption in a linear system. Due to violation of the normality assumption, Wilcoxon Signed-Rank test was used in the analysis. In the β-ratio calculations, we excluded extreme ratio higher than 20 due to low activations (close to zero) in the single occlusion. Furthermore, the average HRF within the activated ROI were plotted from 0 to 18 s after the respiratory occlusion.

Demographic data such as gender, age and education level were recorded and analyzed. Self-reported respiratory sensation rating scores were reported as means ± standard deviations. The paired T-test (with one-tailed threshold) was used to examine the difference in respiratory sensation for the participants between the single- and the paired-occlusion conditions, as it was our a-priori hypothesis that the participants would have experienced higher level of dyspneic sensation in the paired-occlusion condition. One-way analysis of variance (ANOVA) was used to compare the change in mouth pressure elicited by the single-occlusion condition, the first and the second occlusions in the paired-occlusion condition. In the imaging results, we adopted the family-wise error (FWE)-corrected $p < .05$ for significance in the one-sample group results and the 3dClustSim-corrected $p < .05$ (with autocorrelation function) for significance in the between-condition contrast (uncorrected $p < .001$ with cluster threshold = 96 voxels). Wilcoxon Signed-Rank test were performed to compare the effect of occlusions on the estimated beta values for the ROI with the SPSS 19.0 software (SPSS, Inc., Chicago, IL). The significance level was set at $p < .05$.

3. Results

A total of 46 participants' (28 females, mean age = 23.7 ± 3.63 years) data was included in the analysis. Demographic characteristics and self-reported data of the participants are shown in Table 1. All participants had normal lung functions (FEV_1 were at least 70% of predicted values) and none of the participants reported known neurological and cardiorespiratory diseases.

The averaged trial number for the single-occlusion condition was 51 ± 9 (range = 35–71) during the 12-min acquisition time, and that for the paired-occlusion condition was 46 ± 6 (range = 36–60). Change in Pm in the single-occlusion condition was 5.25 ± 1.96 cmH_2O. In the paired-occlusion condition, change in Pm for the S1 and S2 stimuli were 5.48 ± 2.19 and 4.88 ± 2.44 cmH_2O, respectively. One-way ANOVA revealed that there was no significant difference among single occlusion-elicited Pm change, 1st and 2nd occlusion-elicited Pm change in paired occlusion condition (F (2, 135) = 0.86, p = .425, two-tailed). The averaged activation maps for the two respiratory conditions were presented for the main effect of respiratory sensation induced by single and paired

Table 1
Demographic characteristics and pulmonary function test of the participants (N = 46).

Characteristics	*M* ± *SD*
Age (years)	23.70 ± 3.63
Gender (Male / Female)	18 / 28
Education level (high school/ bachelor/master)	5/34/7
FEV_1 (L)	3.19 ± 0.55
$FEV_1{}^{\%}$ predicted	81.8 ± 8.94
FVC (L)	3.41 ± 0.69
FEV_1 / FVC (%)	106 ± 7.95
Self-reported breathlessness (VAS) in single- vs. paired-occlusion condition	28.63 ± 24.41 vs. 32.54 ± 26.32*

FEV_1 = Forced expiratory volume in 1 s; FVC = Forced vital capacity: VAS = Visual Analog Scale ; *p = *.041, one-tailed.*

inspiratory occlusions, showing an overall strong bilateral activation (Fig. 1). The activations of brain regions in response to the single-occlusion condition were found in the caudate nucleus, thalamus, supramarginal gyrus, inferior parietal lobule, left middle frontal gyrus, and left triangular part of inferior frontal gyrus (FWE-corrected, $p < .05$ and cluster size > 20 voxels). For the paired-occlusion condition, significant activations of brain regions were found in the thalamus, amygdala, hippocampus, middle temporal gyrus, inferior frontal gyrus, supramarginal gyrus, cingulate gyrus, postcentral gyrus, supplementary motor area, inferior temporal gyrus and middle frontal gyrus (FWE-corrected, $p < .05$ and cluster size > 20 voxels).

We also found brain regions showing higher activations in response to paired occlusions compared to single occlusion included the temporal gyrus, precentral gyrus, postcentral gyrus, superior temporal gyrus (STG) and thalamus. The activation map of paired occlusion condition compared with single occlusion condition is shown in Fig. 2.

Four ROIs (bilateral basal ganglia, bilateral thalamus, bilateral supramarginal gyrus, and left middle frontal gyrus) were identified as the common brain areas activated during both conditions, and two ROIs (superior temporal and precentral cortices) were determined from the contrast between those two conditions (Fig. 2). The median value of effect size β-values for the bilateral supramarginal gyrus, basal ganglia, thalamus, superior temporal gyrus, precentral cortex and left middle frontal cortex in the single occlusion (Mdn_{single}) were 1.56 [− 2.55 – 4.10], 1.28 [− 1.75 – 5.50], 0.69 [− 3.64 – 4.87], 0.28 [− 3.74 – 3.23], 0.93 [0.04 – 4.19], and 1.09 [− 2.25 – 4.59]; the averaged β-values for the 6 areas in the paired-occlusion condition (Mdn_{paired}) were 1.79 [− 0.59 – 4.68], 1.50 [− 0.57 – 5.53], 1.70 [− 0.65 – 4.23], 1.61 [− 1.66 – 4.47], 1.32 [− 0.63 – 4.18], and 1.23 [− 0.87–4.22], respectively (see Table 2). The medians of β-ratios calculated for the paired- versus single-occlusion conditions ($\beta_{paired}/\beta_{single}$) in the above 6 ROIs were also plotted in Fig. 3. In summary, the Wilcoxon Signed-Rank Test revealed that the β-ratios of the four common areas (basal ganglia, thalamus, and left middle frontal gyrus) were all significantly less than 2 ($Mdn = 0.73$, 0.93, and 0.69; $T = 251$, 252, and 291; $Z = 3.08$, 2.33, and 2.58; $p < .002$, $p = .020$, and $p < .010$, respectively); the β-ratio of supramarginal gyrus was significantly less than 1.5 ($Mdn = 0.91$, $T = 211$, $Z = 3.07$, $p < .002$). The β-ratios for the STG and precentral gyrus have a marginal significance when compared with 2.0 ($Mdn = 1.05$ and 1.07; $T = 280$ and 386; $Z = 1.74$ and 1.87; $p = .082$ and .062, respectively). In addition, the HRF and the time courses of activation were retrieved from the 4 significant ROIs (bilateral thalamus, supramarginal gyrus, basal ganglia and middle frontal gyrus in Fig. 4), delineating the temporal feature underneath the non-linearity between paired- and single-occlusion. Specifically, HRF following single or paired inspiratory occlusions revealed that the supramarginal gyrus and basal ganglia had similar responses between paired and single occlusion conditions. The thalamus and middle frontal gyrus had a relatively higher level of BOLD response in paired- compared to single-occlusion condition. In addition, the thalamus had an earlier peak compared to the other regions.

In terms of dyspnea feeling, the participants rated an overall higher VAS score in the paired- compared with single-occlusion condition (28.63 ± 24.41 vs. 32.54 ± 26.32 for single and paired, respectively; $p = .041$, 1-tailed). The scores for both single- and paired-occlusion conditions ranged from 0 to 90. The Pearson correlation coefficient was used to examine the relationship between scores of dyspnea ratings and β-values. In the single occlusion condition, there was a significant relationship between rated scores of SOB and the β-values in thalamus (r (48) = 0.36, $p = .015$ vs. r (48) = 0.39, $p = .007$ for left and right side, respectively). Fig. 5 presents scatter plots for the β-values of left/right thalamus with the SOB ratings in the single-occlusion condition. There was no significant correlation between dyspnea rating and beta values in the paired-occlusion condition.

4. Discussion

In the present study, our results demonstrated that significant brain activations in response to both paired- and single-occlusion conditions were located in the basal ganglia, thalamus, supramarginal gyrus, and middle frontal gyrus. The neural activation effect size β value ratios βpaired/βsingle) in the above structures were less than 2. Brain areas that were activated significantly more in the paired- compared with single-occlusion condition were the superior temporal gyrus, temporal gyrus, postcentral gyrus, thalamus, and precentral gyrus. In addition, time courses of activation map showed three patterns in the related ROI: (1) four ROIs including the supramarginal gyrus, basal ganglia, thalamus and middle frontal gyrus showed a similar BOLD response pattern between the paired- and single-occlusion conditions; (2) relatively higher activation levels (but still non-linear) in the precentral gyrus and superior temporal regions for paired- compared with single-occlusion condition; (3) the thalamus presented an earlier peak in HRF compared with the above brain regions.

Overall, strong bilateral activations of the cortical structures and subcortical structures confirmed that paired-occlusions were feasible in eliciting neural activations as a function of BOLD responses measured by

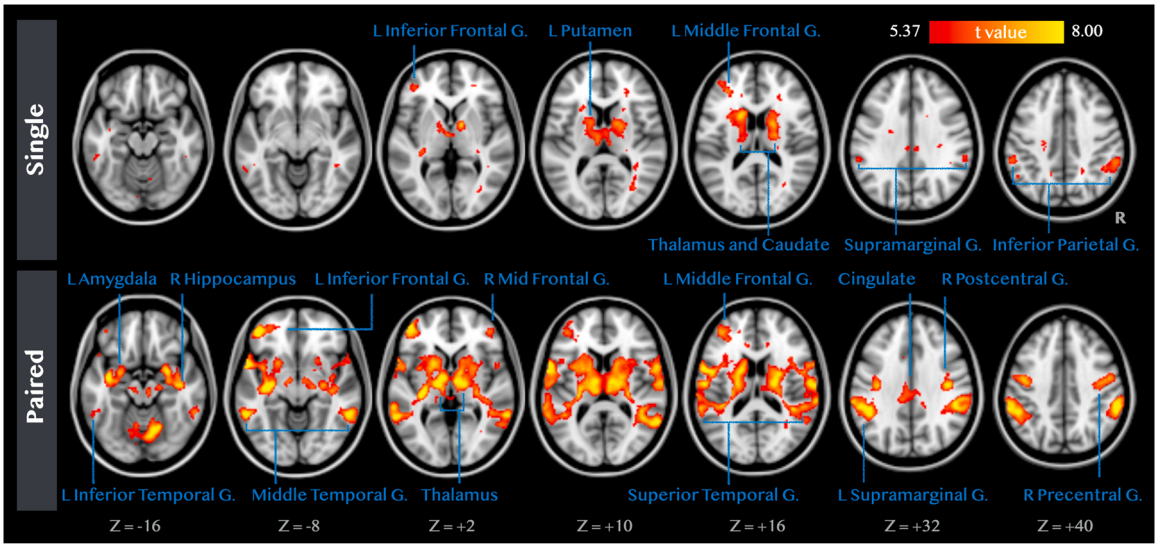

Fig. 1. Group-level brain activations in the axial planes for the single- and the paired-occlusion conditions (N = 46, FWE-corrected $p < .05$ with T-threshold = 5.37).

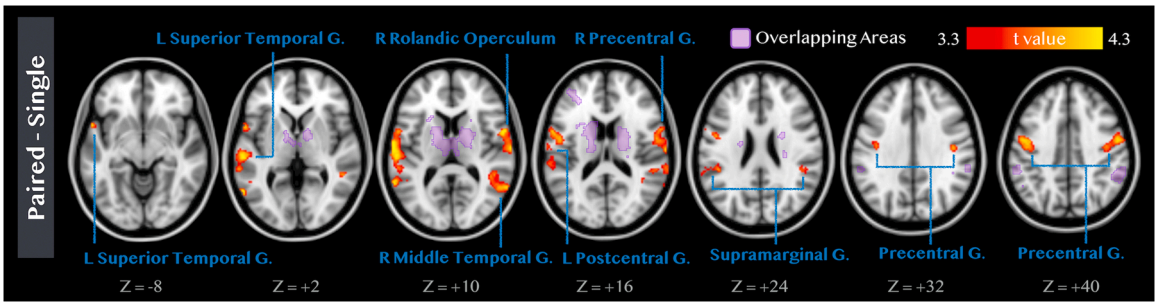

Fig. 2. Between-condition contrast maps in the axial planes for the paired-occlusion condition compared to the single-occlusion condition (3dClusSim-corrected $p < .05$ with T-threshold = 3.3 and cluster threshold = 96 voxels). The purple shaded indicates overlapping areas of brain activations in both single and paired-occlusion conditions.

Table 2
Effect size β-values and β-ratios of neural activations of the 6 ROIs in the single and paired occlusion conditions.

ROI	β Single Occlusion		β Paired Occlusion		β ratio (Paired/Single)		
	Mdn_{single}	Range	Mdn_{paired}	Range	*Mdn*	*T*[a]	*p*-value
Supramarginal G.	1.56	-2.55–4.10	1.79	-0.59–4.68	0.91	114	< .001
Basal Ganglia	1.28	-1.75–5.50	1.50	-0.57–5.53	0.73	251	.002
L Middle Frontal G.	1.09	-2.25–4.59	1.23	-0.87–4.22	0.69	291	.010
Thalamus	0.69	-3.64–4.87	1.70	-0.65–4.23	0.93	252	.020
Superior Temporal G.	0.28	-3.74–3.23	1.61	-1.66–4.47	1.05	280	.082
Precentral G.	0.93	0.04–4.19	1.32	-0.63–4.18	1.07	386	.062

[a] Applying Wilcoxon Signed-Rank test.

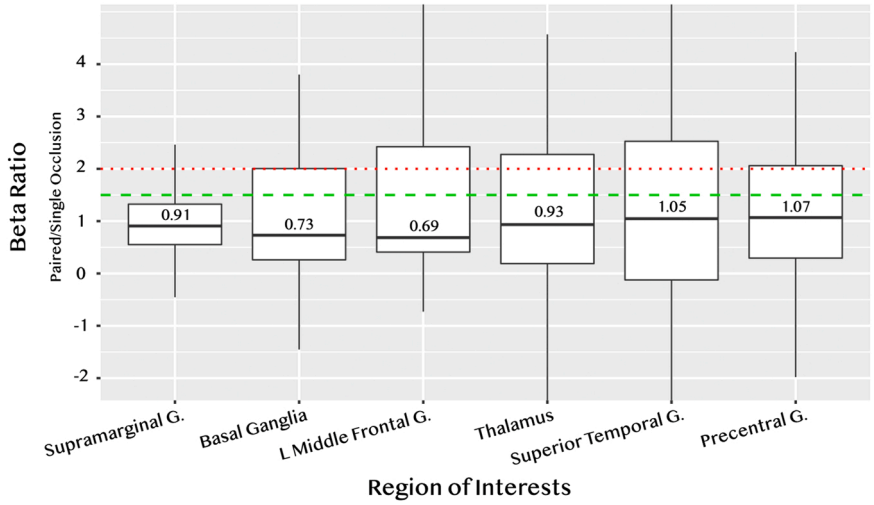

Fig. 3. The beta ratio between the paired and single respiratory occlusions in the six selected regions of interests. The two horizontal lines indicate the reference levels for linearity (Red: beta ratio = 2) and the nonlinearity from previous RREP findings (Green: beta ratio = 1.5).

the fMRI technique. In addition, brain areas activated in single-occlusion condition included the caudate nucleus, thalamus, supramarginal gyrus, inferior parietal lobule, left middle frontal gyrus, and left triangular part of inferior frontal gyrus. These results are consistent with past studies in electrophysiology and neuroimaging examining cerebral neural activations in respiratory sensation (Chan et al., 2019, 2018; von Leupoldt, Chan, Bradley, Lang, & Davenport, 2011; von Leupoldt, Keil, & Davenport, 2011). For example, Chan et al. (2018, 2019) used short inspiratory occlusions as stimulus and found that the thalamus, frontal cortex, caudate, and supramarginal gyrus were significantly activated (Chan et al., 2019, 2018). With high-density EEG technique, von Leupoldt et al. (2011) found that cortical dipoles located in the sensorimotor areas, frontal cortex, and centro-parietal areas were also elicited by inspiratory occlusions (von Leupoldt et al., 2011).

Both the bilateral basal ganglia and thalamus were found to be significantly activated in both single- or paired-occlusion conditions. The role of the thalamus was also confirmed by an animal lesion study, where the thalamic reticular nucleus was found crucial in mediating auditory sensory gating function in rats (Krause, Hoffmann, & Hajos, 2003). In the present study, time course of activation in the thalamus showed a signal change peak earlier than that in the cortical structures including the supramarginal gyrus and precentral gyrus. In addition, the averaged βpaired/βsingle in the basal ganglia and thalamus were approximately 1.2 and 1.1, respectively. Since the β-ratios represent the extent to which paired versus single inspiratory occlusions induced brain structure neural activation, our results suggest that paired occlusion condition induced only slightly higher neural activation compared with single occlusion condition in these subcortical structures. Although it is uncertain which brain substrate serves as the neural "gate" for the paired respiratory stimuli, our time course of activation data (Fig. 4)

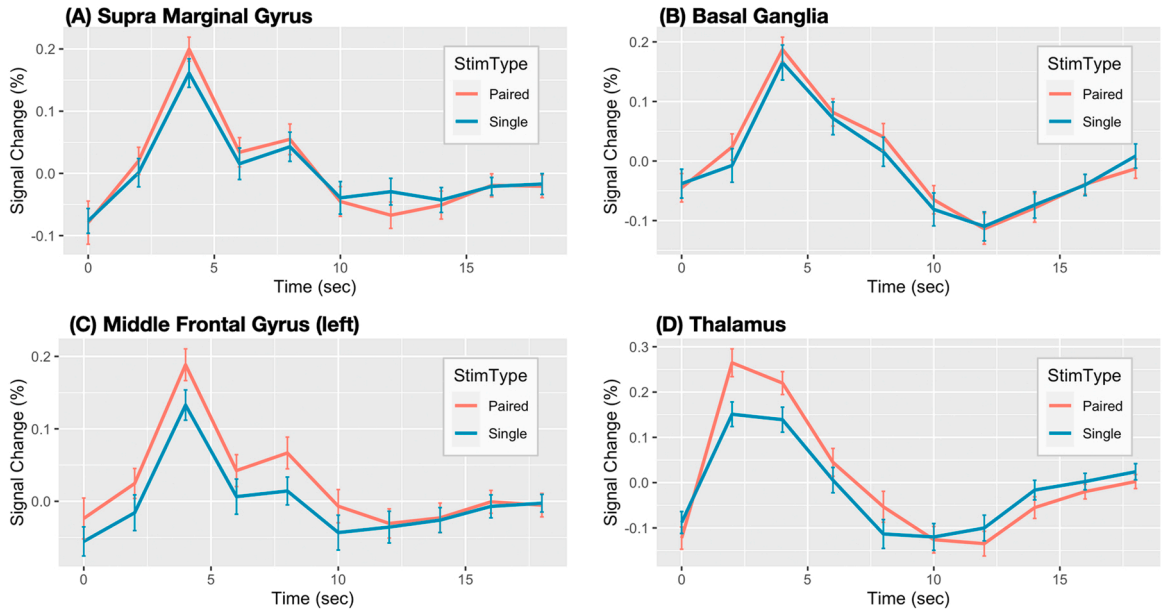

Fig. 4. Temporal hemodynamic responses following single and paired respiratory occlusion in the four common regions. A, B, C, and D presented the temporal curves in the supramarginal gyrus, basal ganglia, left middle frontal gyrus, and thalamus, respectively. The zero second indicates the occlusion onset time.

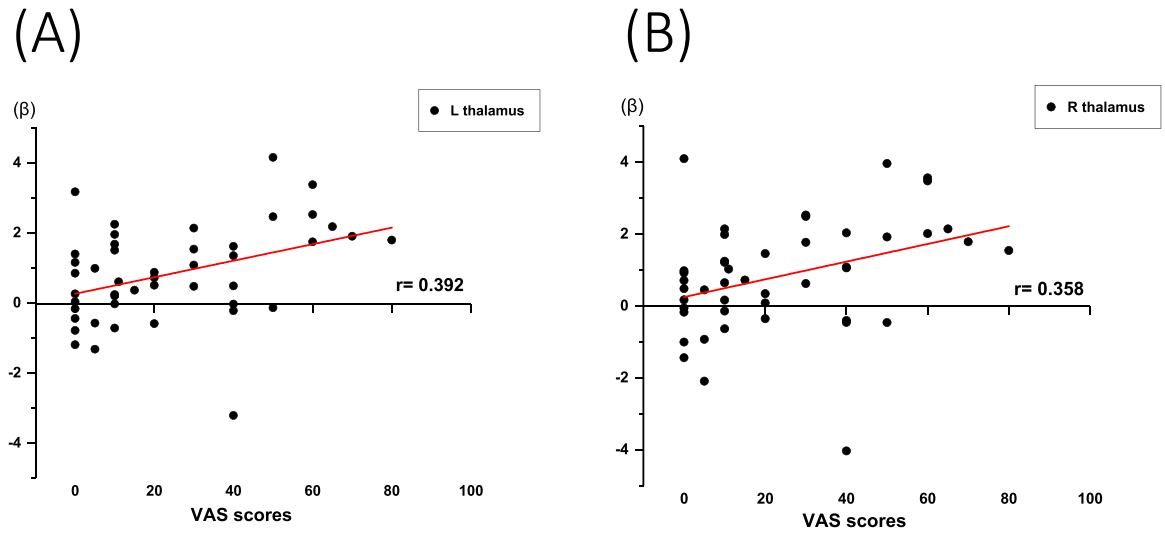

Fig. 5. Scatter plots of the shortness-of-breath VAS ratings and the beta values in the single occlusion condition for the left and right thalamus (A and B, respectively).

supports that respiratory sensory inputs are initially gated at the thalamic level, indicating a threshold gating mechanism.

The middle frontal cortex (MFC) and precentral gyrus emerged as strongly activated areas during paired inspiratory occlusions. A few previous fMRI reports confirmed the role of MFC in dyspnea and loaded breathing (Binks, Evans, Reed, Moosavi, & Banzett, 2014; Chan et al., 2018; Paulus et al., 2012; Stewart, Parnass, May, Davenport, & Paulus, 2013). Additionally, Ruehland, Rochford, Trinder, Spong, and O'Donoghue (2019), who used loads spanning to detect the threshold for eliciting RREPs, reported that even undetected sub-threshold loads can still elicit a RREP Nf peak. Their study suggets that a threshold gating mechanism may exist at the cortical level (Ruehland et al., 2019). Since the premotor and supplementary motor cortex in the MFC receive neural inputs from the primary motor cortex in the precentral gyrus, we reasoned that neural inputs are inhibited at the precentral gyrus, hence subsequent information is processed at a lesser extent in the premotor and/or supplementary motor cortex. Moreover, our results demonstrated that the averaged activation effect size βpaired/βsingle for the MFC was less than 2, suggesting that sensation of the 2nd stimulus was processed at a lesser extent in the MFC. The result seems contrasting to the previous RREP gating studies, which reported that the frontal cortex was significantly activated by the repetitive 2nd stimulus of the paired occlusions (Chan & Davenport, 2008, 2009, 2010a, 2010b; Chan, von Leupoldt, Bradley, Lang, & Davenport, 2012). However, past RREP studies suggested that the frontal cortex to be the origin for not only the Nf peak (Chan & Davenport, 2010a; Logie et al., 1998; Ruehland et al., 2019) but also for the N1 and P2 peaks (von Leupoldt et al., 2010). With our current fMRI setup, we are unable to differentiate whether the neural activation measured in the middle frontal cortex was contributed by only an RREP early peak, or by any later peaks. It is possible that the beta values we retrieved at the frontal area reflected a mixed effect of RREP peaks. Nevertheless, the above evidence, along with our results, support the concept that elements of respiratory sensory information may be gated at the frontal level, and that the frontal lobe may play a role in processing information related to respiratory sensory gating. Future studies with both temporal and spatial resolutions, such as using

the magnetoencephalography technique, are encouraged to overcome this limitation.

The precentral gyrus was activated at a significantly higher level with paired occlusions compared with single occlusion. A possible explanation is that the participants may have experienced higher level of obstructions and put more effort in breathing (load compensation response) during paired occlusions. This was supported by our behavioral data where the participants' ratings of the level of breathlessness in response to paired occlusions were significantly higher than those in response to single occlusion. This higher level of dyspneic feeling may be due to the urge to breathe. Another explanation is that the precentral gyrus could have been activated more in the paired occlusion condition due to voluntary breathing control in response to the expectation of the 2nd respiratory stimulus during breathing. The current event-design in our study is limited to rule out the possibility of the top-down neural recruitment of motor control due to anticipation of the 2nd occlusion. Future studies can perhaps utilize a block design (mixing single with paired occlusions) in the fMRI recording in order to overcome the current limitation.

Additionally, our participants were instructed to breathe as normally as possible throughout the experiment, and to breathe against the obstructions without holding their breaths. This instruction may have involved controlling their breathing consciously and activated the precentral gyrus for controlling volitional movements of the body. This notion is supported by another study where voluntary breathing was found to correlates with elevated brain activities in bilateral sensorimotor areas (McKay, Evans, Frackowiak, & Corfield, 2003). The corresponding neural activation of the movements was therefore recorded by the fMRI scan. Recent work on forebrain descending projections to respiratory control areas suggest that the Kölliker-Fuse nucleus (KFn) in the pons as the gate for medullary command of volitional orofacial behaviors (Dutschmann, Bautista, Trevizan-Bau, Dhingra, & Furuya, 2021; Trevizan-Bau et al., 2020). Trevizan-Bau et al. (2020) found descending neurons from the somatosensory barrel cortex to the KFn in rats (Trevizan-Bau et al., 2020). Furthermore, Dutchsmann et al. (2021) reported that, as a neural gating structure, the KFn sends inhibitory controls to the vagal nerves and induces prolonged inspiration in apneusis (Dutschmann et al., 2021). Although our study design is limited to differentiate whether the neural activation was induced by sensory processes or by voluntary motor movements, the above evidence suggests potential midbrain and subcortical substrates mediating upper- and lower-airway related neural gating.

Areas showing more activations in response to paired-occlusion condition compared to single-occlusion condition including the precentral gyrus, and superior temporal gyrus. This is similar to previous reports that investigated source localization by paired auditory and somatosensory stimuli (Bak et al., 2011, 2014; Grunwald et al., 2003; Mayer et al., 2009). These studies suggest auditory sensory gating are mediated by the temporo-parietal region and frontal cortex. Using a combined EEG and fMRI technique, Bak et al. (2011) reported a few clusters, including medial frontal gyrus and insula, with a 1000 ms minus 500 ms contrast (Bak et al., 2011). On the contrary, there were no clusters identified around the dipole located in the S1 cortex, suggesting that this area is neither involved in P50 generation nor suppression. Although S1 cortex was not identified in neural gating in the study design, we found significant activation in the supramarginal gyrus which is located at the somatosensory association cortex (SII) with paired occlusions. This finding was supported by past electrophysiological studies which showed that SII cortex may mediate secondary information processing after sensory information arrival in the cortex (Chan & Davenport, 2010a; Logie et al., 1998). Together with the βpaired/βsingle being less than 2, our data suggested that the extent to which neural activation in response to the 2nd stimulus is not as robust as the 1st stimulus, supporting the central neural gating mechanism of respiratory sensation.

It is interesting that the thalamus was almost equally activated by the two obstruction conditions, while the precentral gyrus and STG exhibited higher activation in paired occlusion condition. Although our results in the basal ganglia, thalamus, middle frontal gyrus, and supramarginal gyrus suggest that respiratory sensation was gated as a bottom-up process in paired-occlusion condition, the fact that the STG and precentral area were both activated at a much higher level may indicate that some neural processes of cortical activations related to respiratory sensory gating may be top-down controlled. Since the STG is a cortical area in charge of multiple sensory integration process, it could have been recruited for active organizations of neural impulses related to the 2nd stimulus. The above notion is supported by a recent study by Golubic et al. (2019), where they tested the effect of attention on auditory sensory gating with magnetoencephalography and found that attending to the 2nd stimulus significantly changed the gating suppression in the STG component (Golubic et al., 2019). Together, our results implicate that respiratory sensation, similar to other sensations, can be highly affected and integrated by higher cortical interactions including attentional or emotional processes (Chan et al., 2015; Chenivesse et al., 2014; Vuillier et al., 2015).

We also examined the relationships between self-rated breathlessness and ROI. In the single-occlusion condition, scores of breathlessness were positively associated with the activations in the bilateral thalamus. Results in our earlier fMRI studies also supported the results in the present study, suggesting the roles of thalamus in mediating cerebral sensation of respiratory obstructions (Chan et al., 2019, 2018). To note is that although self-reported breathlessness was statistically higher in paired- compared to single-occlusion condition, there was high individual variability within the group. Therefore, this particular finding in the present study is limited for generalization to other studies, and the difference in self-rated dyspnea elicited by single- and paired-occlusion needs further investigation.

There are methodological limitations related to data analysis in the current study. Firstly, with the current setup of fMRI acquisition time of 12 min (in order to accommodate the participants' tolerance to face-mask and inspiratory occlusions in the scanner), the inter-trial-interval (ITI) was not long enough to allow the baseline to be extracted prior to every trial. The ideal ITI for the experiment to determine a stable baseline prior to an occlusion (or occlusion pair) onset would be at least 30 s in time. Thus, we used the initial scans of the first 20 s without the respiratory occlusions as the baseline period to calculate the signal change. Secondly, the inter-trial-interval of 2–4 breaths could be shorter than the observation window of 18-sec in HRF, leading to the possibility that the adjacent HRFs could overlap with each other. However, because the occlusion timing was randomly assigned in each session, the randomized-event design may have highlighted the first HRF and minimize the influence of the second HRF (Miezin, Maccotta, Ollinger, Petersen, & Buckner, 2000). These technical concerns should be carefully addressed in future studies.

In summary, the present study found a non-linear relationship between single- and paired-occlusion elicited brain activations. We demonstrated that the activation effect size in paired-occlusion condition was less than 2 folds of that in single-occlusion condition, suggesting that respiratory sensation is gated at the subcortical and cortical levels. Neural substrates that are closely associated with subcortical and cortical gating of respiratory sensation include the thalamus, basal ganglia, middle frontal gyrus, and supramarginal gyrus. Future research is recommended to examine the effect of physiological and psychological factors on brain substrates in respiratory sensory gating.

Acknowledgement

The authors wish to thank Chia-Wei Li and the National Taiwan University Imaging Center for Integrated Body, Mind, and Culture Research Center for valuable assistance and equipment support. The authors would also like to extend the gratitude to Dr. Susie Huang for the additional proof reading on the manuscript. This study was supported by

MOST-109-2320-B-182-008-MY3 as well as MOST-105-2420-H-182-002-MY3 from the Ministry of Science & Technology in Taiwan, CMRPD1K0081 and BMRPB96 from the Chang Gung Memorial Hospital in Taiwan.

Appendix A. Supporting information

Supplementary data associated with this article can be found in the online version at doi:10.1016/j.biopsycho.2022.108277.

References

Adler, L. E., Pachtman, E., Franks, R. D., Pecevich, M., Waldo, M. C., & Freedman, R. (1982). Neurophysiological evidence for a defect in neuronal mechanisms involved in sensory gating in schizophrenia. *Biological Psychiatry, 17*(6), 639–654. ⟨http://www.ncbi.nlm.nih.gov/entrez/query.fcgi?cmd=Retrieve&db=PubMed&dopt=Citation&list_uids=7104417⟩.

Adler, L. E., & Waldo, M. C. (1991). Counterpoint: A sensory gating–hippocampal model of schizophrenia. *Schizophrenia Bulletin, 17*(1), 19–24. https://doi.org/10.1093/schbul/17.1.19

Arnfred, S. M., Eder, D. N., Hemmingsen, R. P., Glenthoj, B. Y., & Chen, A. C. (2001). Gating of the vertex somatosensory and auditory evoked potential P50 and the correlation to skin conductance orienting response in healthy men. *Psychiatry Research, 101*(3), 221–235. ⟨http://www.ncbi.nlm.nih.gov/entrez/query.fcgi?cmd=Retrieve&db=PubMed&dopt=Citation&list_uids=11311925⟩.

Bak, N., Glenthoj, B. Y., Rostrup, E., Larsson, H. B., & Oranje, B. (2011). Source localization of sensory gating: A combined EEG and fMRI study in healthy volunteers [Research Support, Non-U.S. Gov't]. *Neuroimage, 54*(4), 2711–2718. https://doi.org/10.1016/j.neuroimage.2010.11.039

Bak, N., Rostrup, E., Larsson, H. B., Glenthoj, B. Y., & Oranje, B. (2014). Concurrent functional magnetic resonance imaging and electroencephalography assessment of sensory gating in schizophrenia. *Human Brain Mapping, 35*(8), 3578–3587. https://doi.org/10.1002/hbm.22422

Banzett, R. B., Mulnier, H. E., Murphy, K., Rosen, S. D., Wise, R. J., & Adams, L. (2000). Breathlessness in humans activates insular cortex [Research Support, Non-U.S. Gov't Research Support, U.S. Gov't, P.H.S.]. *Neuroreport, 11*(10), 2117–2120. ⟨http://www.ncbi.nlm.nih.gov/pubmed/10923655⟩.

Binks, A. P., Evans, K. C., Reed, J. D., Moosavi, S. H., & Banzett, R. B. (2014). The time-course of cortico-limbic neural responses to air hunger. *Respiratory Physiology & Neurobiology, 204*, 78–85. https://doi.org/10.1016/j.resp.2014.09.005

Boutros, N. N., Korzyukov, O., Jansen, B., Feingold, A., & Bell, M. (2004). Sensory gating deficits during the mid-latency phase of information processing in medicated schizophrenia patients. *Psychiatry Research, 126*(3), 203–215. https://doi.org/10.1016/j.psychres.2004.01.007

Braff, D. L., & Geyer, M. A. (1990). Sensorimotor gating and schizophrenia. Human and animal model studies. *Archives of General Psychiatry, 47*(2), 181–188. https://doi.org/10.1001/archpsyc.1990.01810140081011

Chan, P. S., Wu, Y. T., Hsu, A. L., Li, C. W., Wu, C. W., von Leupoldt, A., & Hsu, S. C. (2019). The effect of anxiety on brain activation patterns in response to inspiratory occlusions: An fMRI study. *Scientific Reports, 9*(1), 15045. https://doi.org/10.1038/s41598-019-51396-2

Chan, P. Y., Cheng, C. H., Hsu, S. C., Liu, C. Y., Davenport, P. W., & von Leupoldt, A. (2015). Respiratory sensory gating measured by respiratory-related evoked potentials in generalized anxiety disorder [Original Research]. *Frontiers in Psychology*, 6. https://doi.org/10.3389/fpsyg.2015.00957

Chan, P. Y., Cheng, C. H., Wu, Y. T., Wu, C. W., Liu, H. A., Shaw, F. Z., … Davenport, P. W. (2018). Cortical and subcortical neural correlates for respiratory sensation in response to transient inspiratory occlusions in humans. *Frontiers in Physiology, 9*, 1804. https://doi.org/10.3389/fphys.2018.01804

Chan, P. Y., & Davenport, P. W. (2008). Respiratory-related evoked potential measures of respiratory sensory gating. *Journal of Applied Physiology, 105*(4), 1106–1113. ⟨http://www.ncbi.nlm.nih.gov/entrez/query.fcgi?cmd=Retrieve&db=PubMed&dopt=Citation&list_uids=18719232⟩.

Chan, P. Y., & Davenport, P. W. (2009). Respiratory-related-evoked potential measures of respiratory sensory gating in attend and ignore conditions. *Journal of Clinical Neurophysiology, 26*(6), 438–445. ⟨http://www.ncbi.nlm.nih.gov/entrez/query.fcgi?cmd=Retrieve&db=PubMed&dopt=Citation&list_uids=19952570⟩.

Chan, P. Y., & Davenport, P. W. (2010a). Respiratory related evoked potential measures of cerebral cortical respiratory information processing. *Biological Psychology, 84*(1), 4–12. ⟨http://www.ncbi.nlm.nih.gov/entrez/query.fcgi?cmd=Retrieve&db=PubMed&dopt=Citation&list_uids=20188140⟩.

Chan, P. Y., & Davenport, P. W. (2010b). The role of nicotine on respiratory sensory gating measured by respiratory-related evoked potentials. *Journal of Applied Physiology, 108*(3), 662–669. https://doi.org/10.1152/japplphysiol.00798.2009

Chan, P. Y., von Leupoldt, A., Bradley, M. M., Lang, P. J., & Davenport, P. W. (2012). The effect of anxiety on respiratory sensory gating measured by respiratory-related evoked potentials [Research Support, N.I.H., Extramural Research Support, Non-U.S. Gov't]. *Biological Psychology, 91*(2), 185–189. https://doi.org/10.1016/j.biopsycho.2012.07.001

Chenivesse, C., Chan, P. Y., Tsai, H. W., Wheeler-Hegland, K., Silverman, E., von Leupoldt, A., … Davenport, P. (2014). Negative emotional stimulation decreases respiratory sensory gating in healthy humans. *Respiratory Physiology & Neurobiology, 204*, 50–57. https://doi.org/10.1016/j.resp.2014.08.019

Cox, R. W. (1996). AFNI: Software for analysis and visualization of functional magnetic resonance neuroimages. *Computers & Biomedical Research, 29*(3), 162–173. ⟨https://www.ncbi.nlm.nih.gov/pubmed/8812068⟩.

Dale, A. M., & Buckner, R. L. (1997). Selective averaging of rapidly presented individual trials using fMRI. *Human Brain Mapping, 5*(5), 329–340. https://doi.org/10.1002/(SICI)1097-0193(1997)5:5<329::AID-HBM1>3.0.CO;2-5

Davenport, P. W., Colrain, I. M., & Hill, P. M. (1996). Scalp topography of the short-latency components of the respiratory-related evoked potential in children. *Journal of Applied Physiology, 80*(5), 1785–1791. ⟨http://www.ncbi.nlm.nih.gov/entrez/query.fcgi?cmd=Retrieve&db=PubMed&dopt=Citation&list_uids=8727567⟩.

Davenport, P. W., & Vovk, A. (2009). Cortical and subcortical central neural pathways in respiratory sensations. *Respiratory Physiology & Neurobiology, 167*(1), 72–86. https://doi.org/10.1016/j.resp.2008.10.001

Dutschmann, M., Bautista, T. G., Trevizan-Bau, P., Dhingra, R. R., & Furuya, W. I. (2021). The pontine Kolliker-Fuse nucleus gates facial, hypoglossal, and vagal upper airway related motor activity. *Respiratory Physiology & Neurobiology, 284*, Article 103563. https://doi.org/10.1016/j.resp.2020.103563

Freedman, R., Adler, L. E., Myles-Worsley, M., Nagamoto, H. T., Miller, C., Kisley, M., … Waldo, M. (1996). Inhibitory gating of an evoked response to repeated auditory stimuli in schizophrenic and normal subjects. Human recordings, computer simulation, and an animal model. *Archives of Genernal Psychiatry, 53*(12), 1114–1121. https://doi.org/10.1001/archpsyc.1996.01830120052009

Friston, K. J., Josephs, O., Rees, G., & Turner, R. (1998). Nonlinear event-related responses in fMRI. *Magnetic Resonance in Medicine, 39*(1), 41–52. https://doi.org/10.1002/mrm.1910390109

Glover, G. H. (1999). Deconvolution of impulse response in event-related BOLD fMRI. *Neuroimage, 9*(4), 416–429. https://doi.org/10.1006/nimg.1998.0419

Golubic, S. J., Jurasic, M. J., Susac, A., Huonker, R., Gotz, T., & Haueisen, J. (2019). Attention modulates topology and dynamics of auditory sensory gating. *Human Brain Mapping, 40*(10), 2981–2994. https://doi.org/10.1002/hbm.24573

Grunwald, T., Boutros, N. N., Pezer, N., von Oertzen, J., Fernandez, G., Schaller, C., & Elger, C. E. (2003). Neuronal substrates of sensory gating within the human brain. *Biological Psychiatry, 53*(6), 511–519. https://doi.org/10.1016/s0006-3223(02)01673-6

Huettel, S. A., & McCarthy, G. (2000). Evidence for a refractory period in the hemodynamic response to visual stimuli as measured by MRI. *Neuroimage, 11*(5 Pt 1), 547–553. https://doi.org/10.1006/nimg.2000.0553

Inan, S., Mitchell, T., Song, A., Bizzell, J., & Belger, A. (2004). Hemodynamic correlates of stimulus repetition in the visual and auditory cortices: an fMRI study. *Neuroimage, 21*(3), 886–893. https://doi.org/10.1016/j.neuroimage.2003.10.029

Jack, S., Kemp, G. J., Bimson, W. E., Calverley, P. M., & Corfield, D. R. (2010). Patterns of brain activity in response to respiratory stimulation in patients with idiopathic hyperventilation (IHV). *Advances in Experimental Medicine & Biology, 669*, 341–345. https://doi.org/10.1007/978-1-4419-5692-7_70

Jelincic, V., Torta, D. M., Van Diest, I., & von Leupoldt, A. (2021). Cross-modal relationships of neural gating with the subjective perception of respiratory and somatosensory sensations. *Psychophysiology, 58*(1), Article e13710. https://doi.org/10.1111/psyp.13710

Korzyukov, O., Pflieger, M. E., Wagner, M., Bowyer, S. M., Rosburg, T., Sundaresan, K., … Boutros, N. N. (2007). Generators of the intracranial P50 response in auditory sensory gating. *Neuroimage, 35*(2), 814–826. https://doi.org/10.1016/j.neuroimage.2006.12.011

Krause, M., Hoffmann, W. E., & Hajos, M. (2003). Auditory sensory gating in hippocampus and reticular thalamic neurons in anesthetized rats. *Biological Psychiatry, 53*(3), 244–253. https://doi.org/10.1016/s0006-3223(02)01463-4

von Leupoldt, A., Chan, P. Y., Bradley, M. M., Lang, P. J., & Davenport, P. W. (2011). The impact of anxiety on the neural processing of respiratory sensations. https://doi.org/S1053-8119(10)01528-4 [pii] *Neuroimage, 55*(1), 247–252. https://doi.org/10.1016/j.neuroimage.2010.11.050.

von Leupoldt, A., Keil, A., Chan, P. Y., Bradley, M. M., Lang, P. J., & Davenport, P. W. (2010). Cortical sources of the respiratory-related evoked potential. https://doi.org/S1569-9048(09)00376-0 [pii] *Respiratory Physiology & Neurobiology, 170*(2), 198–201. https://doi.org/10.1016/j.resp.2009.12.006.

von Leupoldt, A., Keil, A., & Davenport, P. W. (2011). Respiratory-related evoked potential measurements using high-density electroencephalography. *Clinical Neurophysiology, 122*(4), 815–818. https://doi.org/10.1016/j.clinph.2010.10.031

von Leupoldt, A., Sommer, T., Kegat, S., Baumann, H. J., Klose, H., Dahme, B., & Buchel, C. (2008). The unpleasantness of perceived dyspnea is processed in the anterior insula and amygdala. *American Journal of Respiratory & Critical Care Medicine, 177*(9), 1026–1032. ⟨http://www.ncbi.nlm.nih.gov/entrez/query.fcgi?cmd=Retrieve&db=PubMed&dopt=Citation&list_uids=18263796⟩.

von Leupoldt, A., Sommer, T., Kegat, S., Eippert, F., Baumann, H. J., Klose, H., … Buchel, C. (2009). Down-regulation of insular cortex responses to dyspnea and pain in asthma. *American Journal of Respiratory & Critical Care Medicine, 180*(3), 232–238. https://doi.org/10.1164/rccm.200902-0300OC

Logie, S. T., Colrain, I. M., & Webster, K. E. (1998). Source dipole analysis of the early components of the RREP. *Brain Topography, 11*(2), 153–164. ⟨http://www.ncbi.nlm.nih.gov/entrez/query.fcgi?cmd=Retrieve&db=PubMed&dopt=Citation&list_uids=9880173⟩.

Manning, H. L., Shea, S. A., Schwartzstein, R. M., Lansing, R. W., Brown, R., & Banzett, R. B. (1992). Reduced tidal volume increases "air hunger" at fixed PCO2 in ventilated quadriplegics. *Respiratory Physiology, 90*(1), 19–30. ⟨https://www.ncbi.nlm.nih.gov/pubmed/1455095⟩.

Mayer, A. R., Hanlon, F. M., Franco, A. R., Teshiba, T. M., Thoma, R. J., Clark, V. P., & Canive, J. M. (2009). The neural networks underlying auditory sensory gating [Research Support, N.I.H., Extramural Research Support, U.S. Gov't, Non-P.H.S.]. *Neuroimage, 44*(1), 182–189. https://doi.org/10.1016/j.neuroimage.2008.08.025

McKay, L. C., Evans, K. C., Frackowiak, R. S., & Corfield, D. R. (2003). Neural correlates of voluntary breathing in humans. *Journal of Applied Physiology, 95*(3), 1170–1178. https://doi.org/10.1152/japplphysiol.00641.2002

Miezin, F. M., Maccotta, L., Ollinger, J. M., Petersen, S. E., & Buckner, R. L. (2000). Characterizing the hemodynamic response: Effects of presentation rate, sampling procedure, and the possibility of ordering brain activity based on relative timing. *Neuroimage, 11*(6 Pt 1), 735–759. https://doi.org/10.1006/nimg.2000.0568

Moosavi, S. H., Golestanian, E., Binks, A. P., Lansing, R. W., Brown, R., & Banzett, R. B. (2003). Hypoxic and hypercapnic drives to breathe generate equivalent levels of air hunger in humans. *Journal of Appled Physiology, 94*(1), 141–154. https://doi.org/10.1152/japplphysiol.00594.2002

Paulus, M. P., Flagan, T., Simmons, A. N., Gillis, K., Kotturi, S., Thom, N., … Swain, J. L. (2012). Subjecting elite athletes to inspiratory breathing load reveals behavioral and neural signatures of optimal performers in extreme environments. *PLoS One, 7*(1), Article e29394. https://doi.org/10.1371/journal.pone.0029394

Peiffer, C., Costes, N., Herve, P., & Garcia-Larrea, L. (2008). Relief of dyspnea involves a characteristic brain activation and a specific quality of sensation. *American Journal of Respiratory & Critical Care Medicine, 177*(4), 440–449. https://doi.org/10.1164/rccm.200612-1774OC

Peiffer, C., Poline, J. B., Thivard, L., Aubier, M., & Samson, Y. (2001). Neural substrates for the perception of acutely induced dyspnea [Clinical Trial Comparative Study]. *American Journal of Respiratory & Critical Care Medicine, 163*(4), 951–957. ⟨http://www.ncbi.nlm.nih.gov/pubmed/11282772⟩.

Rentzsch, J., Jockers-Scherubl, M. C., Boutros, N. N., & Gallinat, J. (2008). Test-retest reliability of P50, N100 and P200 auditory sensory gating in healthy subjects. *International Journal of Psychophysiology, 67*(2), 81–90. https://doi.org/10.1016/j.ijpsycho.2007.10.006

Ruehland, W. R., Rochford, P. D., Trinder, J., Spong, J., & O'Donoghue, F. J. (2019). Evidence against a subcortical gate preventing conscious detection of respiratory load stimuli. *Respiratory Physiology & Neurobiology, 259*, 93–103. https://doi.org/10.1016/j.resp.2018.08.005

Shen, C. L., Chou, T. L., Lai, W. S., Hsieh, M. H., Liu, C. C., Liu, C. M., & Hwu, H. G. (2020). P50, N100, and P200 auditory sensory gating deficits in schizophrenia patients. *Frontiers in Psychiatry, 11*, 868. https://doi.org/10.3389/fpsyt.2020.00868

Stewart, J. L., Parnass, J. M., May, A. C., Davenport, P. W., & Paulus, M. P. (2013). Altered frontocingulate activation during aversive interoceptive processing in young adults transitioning to problem stimulant use. *Frontiers in Systems Neuroscience, 7*, 89. https://doi.org/10.3389/fnsys.2013.00089

Thoma, L., Rentzsch, J., Gaudlitz, K., Tanzer, N., Gallinat, J., Kathmann, N., … Plag, J. (2020). P50, N100, and P200 sensory gating in panic disorder. *Clinical EEG & Neuroscience, 51*(5), 317–324. https://doi.org/10.1177/1550059419899324

Thoma, R. J., Hanlon, F. M., Huang, M., Miller, G. A., Moses, S. N., Weisend, M. P., … Canive, J. M. (2007). Impaired secondary somatosensory gating in patients with schizophrenia. *Psychiatry Research, 151*(3), 189–199. https://doi.org/10.1016/j.psychres.2006.10.011

Trevizan-Bau, P., Dhingra, R. R., Furuya, W. I., Stanic, D., Mazzone, S. B., & Dutschmann, M. (2020). Forebrain projection neurons target functionally diverse respiratory control areas in the midbrain, pons, and medulla oblongata. *Journal of Comparative Neurology*. https://doi.org/10.1002/cne.25091

Vuillier, L., Hermens, D. F., Chitty, K., Wang, C., Kaur, M., Ward, P. B., … Lagopoulos, J. (2015). Emotional processing, p50 sensory gating, and social functioning in bipolar disorder. *Clinical EEG & Neuroscience, 46*(2), 81–87. https://doi.org/10.1177/1550059414523417

Webster, K. E., & Colrain, I. M. (1998). Multichannel EEG analysis of respiratory evoked-potential components during wakefulness and NREM sleep. *Journal of Applied Physiology, 85*(5), 1727–1735. https://doi.org/10.1152/jappl.1998.85.5.1727

Webster, K. E., & Colrain, I. M. (2000). The respiratory-related evoked potential: Effects of attention and occlusion duration. *Psychophysiology, 37*(3), 310–318. ⟨http://www.ncbi.nlm.nih.gov/entrez/query.fcgi?cmd=Retrieve&db=PubMed&dopt=Citation&list_uids=10860409⟩.